

Sub-barrier fusion enhancement in neutron-rich radioactive ^{132}Sn on ^{64}Ni

J. F. LIANG¹, D. SHAPIRA¹, C. J. GROSS¹, J. R. BEENE¹, J. D. BIERMAN²,
A. GALINDO-URIBARRI¹, J. GOMEZ DEL CAMPO¹, P. A. HAUSLADEN¹,
Y. LAROCHELLE³, W. LOVELAND⁴, P. E. MUELLER¹, D. PETERSON⁴,
D. C. RADFORD¹, D. W. STRACENER¹, and R. L. VARNER¹

¹*Physics Division, Oak Ridge National Laboratory, Oak Ridge, Tennessee 37831,
USA*

²*Physics Department AD-51, Gonzaga University, Spokane, Washington
99258-0051, USA*

³*Department of Physics and Astronomy, University of Tennessee, Knoxville,
Tennessee 37966, USA*

⁴*Department of Chemistry, Oregon State University, Corvallis, Oregon 97331, USA*

Evaporation residue cross sections have been measured using neutron-rich radioactive ^{132}Sn beams incident on a ^{64}Ni target in the vicinity of the Coulomb barrier. This is the first experiment using accelerated ^{132}Sn beams to study nuclear reaction mechanisms. The average beam intensity was 2×10^4 particles per second and the smallest cross section measured was less than 5 mb. A large sub-barrier fusion enhancement was observed compared to evaporation residue cross sections for ^{64}Ni on stable even Sn isotopes. The enhancement cannot be accounted for by a simple barrier shift due to the change in nuclear sizes. Coupled-channel calculations including inelastic excitation underpredict the measured cross sections below the barrier. The presence of several neutron transfer channels with large positive Q values suggests that multinucleon transfer may play an important role in enhancing the fusion of ^{132}Sn and ^{64}Ni .

§1. Introduction

Enhanced sub-barrier fusion cross sections have been found in many heavy ion reactions. The enhancement can be described in most cases by the coupling of the relative motion and the nuclear structure degrees of freedom of the participating nuclei.¹⁾ It has been suggested that the fusion yield would be further enhanced when the reaction is induced by radioactive neutron-rich nuclei.²⁾⁻⁴⁾ This is attributed to the large N/Z ratio of these nuclei reducing the barrier height and the presence of a large number of nucleon transfer channels which can serve as doorway states to fusion.⁵⁾ If the predictions were verified to be correct, using neutron-rich radioactive beams can be an alternative way for producing superheavy elements. Additionally, using a closed shell neutron-rich projectile, such as ^{132}Sn , and target will lead to compound systems with lower excitation energies and with a smaller fissility and, therefore, a higher survival probability.⁶⁾

The search for fusion enhancement using neutron-rich radioactive beams has been pursued in several laboratories. The measurements of $^{38}\text{S}+^{181}\text{Ta}$ ⁷⁾ and $^{29,31}\text{Al}+^{197}\text{Au}$ ⁸⁾ found only the enhancement expected from the lowering of the barrier height caused by the larger radii of the neutron-rich nuclei compared to the

stable ^{32}S and ^{27}Al , respectively. This paper reports the first measurement of evaporation residue (ER) cross sections using accelerated unstable neutron-rich ^{132}Sn beams. The doubly magic ^{132}Sn ($Z=50$, $N=82$) has eight extra neutrons compared to the heaviest stable Sn isotope, ^{124}Sn . The N/Z ratio of ^{132}Sn (1.64) is larger than that of ^{48}Ca (1.4) and ^{208}Pb (1.54) which are closed shell nuclei commonly used in heavy element production.⁹⁾

§2. Experimental methods

The measurements were performed at the Holifield Radioactive Ion Beam Facility (HRIBF) at Oak Ridge National Laboratory. Short-lived ^{132}Sn was produced from proton-induced uranium fission using the isotope separator on-line technique. Isobars of mass $A=132$ were suppressed by extracting molecular SnS^+ from the ion source and subsequently breaking it up in the charge exchange cell where the SnS^+ was converted to Sn^- .¹⁰⁾ The ^{132}Sn ions were post accelerated by the 25 MV tandem electrostatic accelerator. The beam intensity was measured by passing it through a $10\ \mu\text{g}/\text{cm}^2$ carbon foil and detecting the secondary electrons in a microchannel plate (MCP) detector. The average beam intensity was 2×10^4 particles per second (pps) with a maximum near 3×10^4 pps. The purity of the ^{132}Sn beam was determined by measuring the energy loss in an ionization chamber and the contaminants were less than 2%. Moreover, all the measurable impurities had a higher atomic number (Z) than Sn. (Lower Z isobars have much shorter lifetimes and, therefore, less chance of getting out of the ion source.) This impurity has negligible influence on the measurement because the higher Coulomb barrier suppresses the fusion of the contaminants with the target. Because of the low intensity of radioactive beams, the measurement was performed with a thick, $1\ \text{mg}/\text{cm}^2$, self-supporting highly enriched (99.8%) ^{64}Ni foil target. A ^{124}Sn beam was used as a guide beam to set up the accelerator and beamline optics, and test the detector system.

The ERs were detected along with beam particles by a timing detector and an ionization chamber at 0° , as shown in Fig. 1. They were identified by their time-of-flight and energy loss in the ionization chamber. In the time-of-flight measurement, the coincidence between the two upstream timing detectors provided the timing references. The data acquisition was triggered by the scaled down beam singles or the ER-beam particle coincidences. With this triggering scheme an overall deadtime of less than 5% and measurement of ER cross sections less than 5 mb can be achieved.

§3. Data reduction and results

The ERs were very forward focused because of the inverse kinematics. However, one of the disadvantages of using a thick target is the multiple scattering which results in broadening the angular distribution. The efficiency of the apparatus was estimated by Monte Carlo simulations using the statistical model code PACE¹¹⁾ to generate the angular distribution of ERs. The efficiency of the apparatus changes from $95 \pm 1\%$ for the lowest beam energy to $98 \pm 1\%$ for the highest energy.

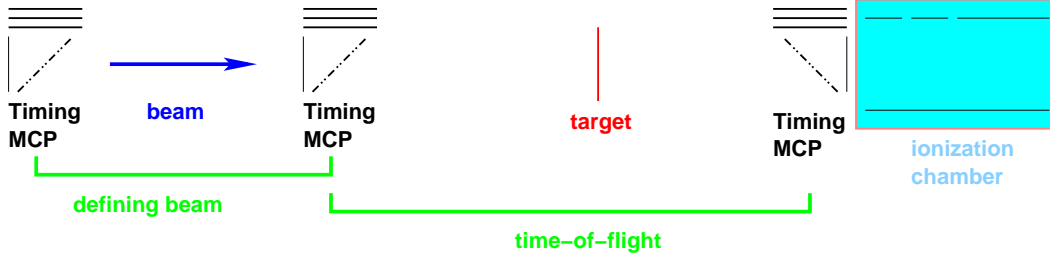
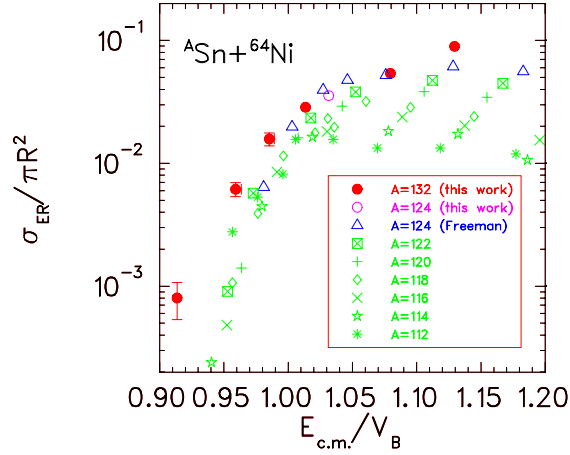


Fig. 1. Schematic of the experimental apparatus.

The ER excitation function for $^{132}\text{Sn}+^{64}\text{Ni}$ (solid circles) is compared to those of ^{64}Ni on even Sn isotopes measured by Freeman *et al.*¹²⁾ in Fig. 2. Our measurement using the ^{124}Sn guide beam is shown by the open circle and agrees well with the measurement of Ref. 12) as shown by the open triangles. In Fig. 2 the energy is scaled by the fusion barrier (V_B) predicted by the Bass model¹³⁾ and the ER cross section is scaled by the size of the reactants using $R = 1.2(A_p^{1/3} + A_t^{1/3})$ fm, where A_p and A_t are the mass of the projectile and target, respectively. At energies below the barrier, the ER cross sections for $^{132}\text{Sn}+^{64}\text{Ni}$ are found much enhanced compared to those of $^{64}\text{Ni}+^{112-124}\text{Sn}$ and a simple shift of the barrier height cannot explain the enhancement.


 Fig. 2. Fusion-evaporation excitation functions of $^{132}\text{Sn}+^{64}\text{Ni}$ (filled circles) and ^{64}Ni on even $^{112-124}\text{Sn}$.¹²⁾ The open circle is our measurement using a ^{124}Sn beam.

§4. Discussion

To compare the measured excitation function with fusion models, it is necessary to estimate the fission contribution since it was not measured in our experiment. The estimate was carried out by statistical model calculations using the code PACE. The input parameters were determined by reproducing the ER and fission cross sections

for $^{64}\text{Ni}+^{124}\text{Sn}$ in Ref. 14). The calculations predicted that fission is negligible for $^{64}\text{Ni}+^{124}\text{Sn}$ and $^{132}\text{Sn}+^{64}\text{Ni}$ at $E_{\text{c.m.}} \leq 160$ MeV. Therefore, the following discussion will be restricted to the data points at $E_{\text{c.m.}} \leq 160$ MeV where the ER cross sections are taken as fusion cross sections.

As reported in Ref. 15), large sub-barrier fusion enhancement was observed for both $^{132}\text{Sn}+^{64}\text{Ni}$ and $^{64}\text{Ni}+^{124}\text{Sn}$ when the measured excitation functions were compared to the one-dimensional barrier penetration model. The potential parameters for the barrier penetration model were obtained from calculations reproducing the fusion cross section for $^{64}\text{Ni}+^{124}\text{Sn}$ at high energies. Coupled-channel calculations including inelastic excitation of the projectile and target were performed with the code CCFULL.¹⁶⁾ The calculation reproduced the $^{64}\text{Ni}+^{124}\text{Sn}$ cross sections fairly well at low energies whereas for $^{132}\text{Sn}+^{64}\text{Ni}$ the calculation significantly underpredicted the sub-barrier cross sections, as can be seen in Fig. 3 of Ref. 15).

For the ^{132}Sn -induced reaction, the Q values are positive for ^{64}Ni picking up two to six neutrons whereas in $^{64}\text{Ni}+^{124}\text{Sn}$, the ($^{64}\text{Ni}, ^{66}\text{Ni}$) reaction is the only transfer channel which has a positive Q value. This suggests that the observed fusion enhancement may be attributed to multinucleon transfer similar to that observed in $^{40}\text{Ca}+^{96}\text{Zr}$.¹⁷⁾ Coupled-channel calculations including the ($^{64}\text{Ni}, ^{66}\text{Ni}$) neutron transfer channel and inelastic excitation are in good agreement with the fusion cross sections for $^{64}\text{Ni}+^{124}\text{Sn}$ near and below the barrier. The calculation including inelastic excitation, and multinucleon transfer channels assuming clusters of neutrons transferred to the ground state cannot account for the cross sections for $^{132}\text{Sn}+^{64}\text{Ni}$ near and below the barrier.¹⁵⁾ It is noted that the code CCFULL is suitable for reactions where multinucleon transfer is less important than inelastic excitation¹⁶⁾ as is the case in $^{64}\text{Ni}+^{124}\text{Sn}$.

To further explore the effects of coupling to the transfer channels, we have included neutrons transferred to the excited states of the daughter nuclei in the calculations and used a modified version of CCMOD.¹⁸⁾ The coupling scheme is similar to that illustrated in Fig. 1 of Ref. 19). The one-neutron transfer form factor was parameterized as²⁰⁾

$$F_{1n}(r) = F_0^{(1n)} \frac{e^{-\alpha r}}{\alpha r},$$

where the α is the slope of the transfer probability at large distances. The slope parameter, α , and the coupling constant, $F_0^{(1n)}$, for $^{58}\text{Ni}+^{124}\text{Sn}$ were extracted from the measurement by C. L. Jiang *et al.*²¹⁾ Following the prescription given in Ref. 19), the form factors for successive one-neutron transfer were

$$F_{2n,1n}(r) = \sqrt{2}F_{1n}(r)$$

and

$$F_{3n,2n}(r) = \sqrt{3/2}F_{1n}(r).$$

The transfer form factor for pair-neutron transfer was parameterized as

$$F_{2n}(r) = F_0^{(2n)} e^{-(r-r_0)/1.2},$$

where $F_0^{(2n)}$ was arbitrarily set to 1.0 and $r_0 = 1.2(A_p^{1/3} + A_t^{1/3})$. The results of calculations including inelastic excitation of the projectile and target, two-phonon excitation, mutual excitation, and transfer of up to three neutrons for $^{58}\text{Ni}+^{124}\text{Sn}$ are shown by the solid curve in Fig. 3. It can be seen that the experimental fusion cross sections are well reproduced by the calculation. Similar calculations performed for $^{64}\text{Ni}+^{124}\text{Sn}$ but including the one transfer channel with positive Q value are also in good agreement with the measurement, as shown in the right panel of Fig. 4. For $^{132}\text{Sn}+^{64}\text{Ni}$, the slope parameter,²⁰⁾ $\alpha \propto \sqrt{\mu B_n}$, was scaled by the neutron binding energy (B_n) and the reduced mass (μ). Shown in left panel of Fig. 4 are the results of the calculations. The dashed curve is the calculation without considering transfer and the solid curve is the calculation including transfer of up to three neutrons. As can be seen, even the calculation including the coupling to neutron transfer channels underpredicts the measurement. It should be pointed out that the nuclear potential used in this calculation was taken to be the same as that for $^{64}\text{Ni}+^{124}\text{Sn}$ and was not adjusted. Measurements of fusion cross sections at energies above the barrier are needed to obtain the potential parameters which may improve the calculation and reduce the discrepancy between the calculation and measurement. Moreover, measuring transfer channels would provide useful information on the transfer form factor.

It can be seen in Fig. 2 that at the highest energy the ER cross section for $^{132}\text{Sn}+^{64}\text{Ni}$ is larger than that for other Sn isotopes. This can be expected from the higher stability against fission for the neutron-rich compound nucleus. Further experiments are planned to measure fission in $^{132}\text{Sn}+^{64}\text{Ni}$ at higher energies to study the survival probability of the compound nucleus.

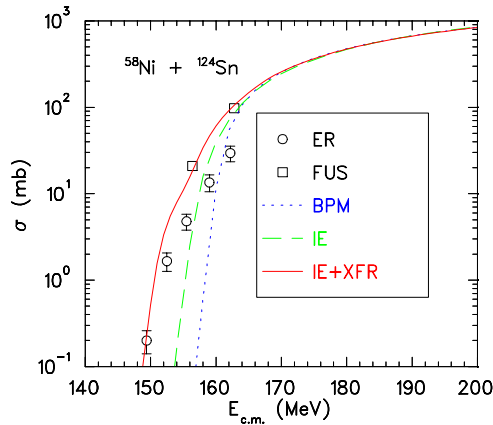


Fig. 3. Comparison of measured $^{58}\text{Ni}+^{124}\text{Sn}$ ER excitation functions¹²⁾ with CCMOD calculations. The measured ER cross sections are shown by the open circles and the fusion cross sections are shown by the open squares. The result of a one-dimensional barrier penetration model prediction is shown by the dotted curve. The coupled-channel calculations including inelastic excitation, and inelastic excitation and transfer are shown by the dashed and solid curves, respectively.

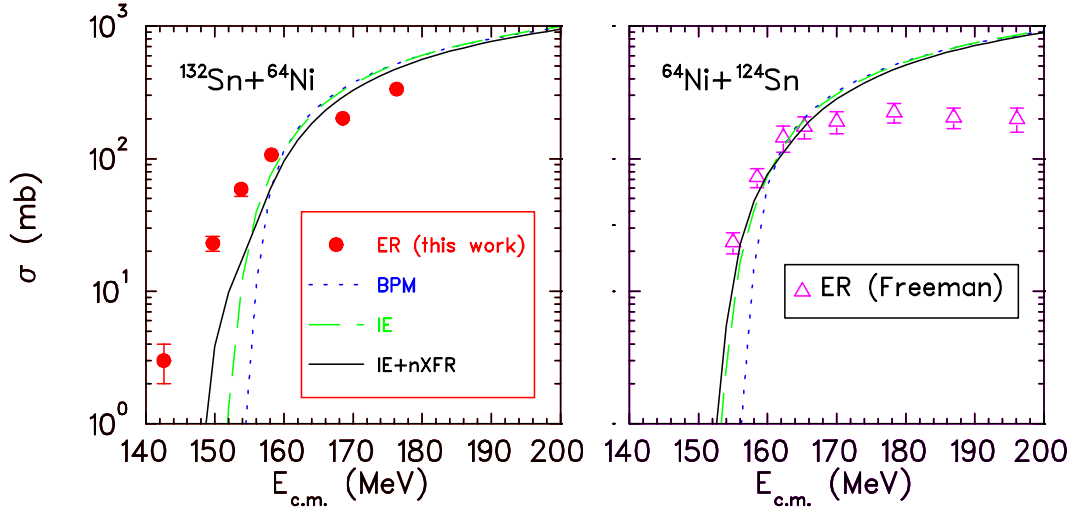


Fig. 4. Comparison of measured ER excitation functions with CCMOD calculations. The left panel is for $^{132}\text{Sn}+^{64}\text{Ni}$ and the right panel is for $^{64}\text{Ni}+^{124}\text{Sn}$.¹²⁾ The measured ER cross sections are shown by the filled circles and open triangles for $^{132}\text{Sn}+^{64}\text{Ni}$ and $^{64}\text{Ni}+^{124}\text{Sn}$, respectively. The calculations including inelastic excitation, and inelastic excitation and transfer are shown by the dashed and solid curves, respectively.

§5. Summary and outlook

Evaporation residue cross sections using neutron-rich radioactive ^{132}Sn beams on a ^{64}Ni target were measured at energies near the Coulomb barrier. A large sub-barrier fusion enhancement was observed. The enhancement cannot be explained by a simple shift of the barrier height due to the change in nuclear sizes, or by the coupling to inelastic excitation channels. The presence of several neutron transfer channels with positive Q values may serve as doorway states to fusion. To further our study, preparation for experiments using even more neutron-rich radioactive ^{134}Sn beams is underway. The reaction energies were near and below the Coulomb barrier in this experiment. We plan to extend the measurement of the same reaction system to higher energies where the decay of the compound nucleus by fission becomes significant to study the influence of neutron excess on survival probability.

Acknowledgements

We wish to thank the HRIBF staff for providing excellent radioactive beams and technical support. One of us (JFL) wish to thank M. Dasgupta, H. Esbensen, K. Hagino, and F. M. Nunes for fruitful discussions on coupled-channel calculations. Research at the Oak Ridge National Laboratory is supported by the U.S. Department of Energy under contract DE-AC05-00OR22725 with UT-Battelle, LLC. W. Loveland and D. Peterson are supported by the the U.S. Department of Energy under grant no. DE-FG06-97ER41026.

References

- 1) M. Beckerman, Rep. Prog. Phys. **51** (1988) 1047.
- 2) N. Takigawa, H. Sagawa, and T. Shinozuka, Nucl. Phys. A **538** (1992) 221c.
- 3) M. S. Hussein, Nucl. Phys. A **531** (1991) 192.
- 4) C. H. Dasso and R. Donangelo, Phys. Lett. B **276** (1992) 1.
- 5) V. Yu. Denisov, Eur. Phys. J. A **7** (2000) 87.
- 6) S. Hofmann, Prog. Part. Nucl. Phys. **46** (2001) 293.
- 7) K. E. Zyromski *et al.*, Phys. Rev. C **55** (1997) R562.
- 8) C. Signorini, Nucl. Phys. A **693** (2001) 190.
- 9) S. Hofmann and G. Münzenberg, Rev. Mod. Phys. **72** (2000) 733.
- 10) D. W. Stracener, Nucl. Instrum. and Methods Phys. Res., Sect. B **204** (2003) 42.
- 11) A. Gavron, Phys. Rev. C **21** (1980) 230.
- 12) W. S. Freeman *et al.*, Phys. Rev. Lett. **50** (1983) 1563.
- 13) R. Bass, Nucl. Phys. A **231** (1974) 45.
- 14) K. T. Lesko *et al.*, Phys. Rev. C **34** (1986) 2155.
- 15) J. F. Liang *et al.*, Phys. Rev. Lett. **91** (2003), 152701.
- 16) K. Hagino, N. Rowley, and A. T. Kruppa, Compu. Phys. Commun. **123** (1999) 143.
- 17) H. Timmers *et al.*, Nucl. Phys. A **633** (1998) 421.
- 18) M. Dasgupta *et al.*, Nucl. Phys. A **A539** (1992), 351.
- 19) H. Esbensen, C. L. Jiang, and K. E. Rehm, Phys. Rev. C **57** (1998), 2401.
- 20) L. Corradi *et al.*, Z. Phys. A **334** (1990) 55.
- 21) C. L. Jiang *et al.*, Phys. Rev. C **57** (1998), 2393.